Spiking Cortical Model for Rotation and Scale Invariant Texture Retrieval

Kun Zhan, Jicai Teng, Yide Ma

School of Information Science and Engineering, Lanzhou University, Lanzhou Gansu 730000, China
Email: kzhan@lzu.edu.cn, Tel: 13609370924, Fax, 86-931-8912778

ABSTRACT. *Retrieval of texture images, especially those with different orientation and scale changes, is a challenging and important problem in image analysis. This paper adopts spiking cortical model (SCM) to explore geometrical invariant texture retrieval schemes based on Discrete Cosine Transform (DCT) coefficients of pulse images. The series of pulse images, outputs of SCM, have a robust talent for extracting edge, segment and texture which are inherent in the original images, but they are large 2-dimensional image data so that it is difficult to process further. Geometrical invariant features of the original images can be extracted by characterizing the pulse images in DCT domain, which is dramatically reduced the large data to a small 1-dimensional vector. Many experiments and comparative studies are performed to show that the retrieval schemes are novel and effective in extracting invariant features.*
Keywords: Invariance; Spiking Cortical Model; Texture Retrieval; Discrete cosine transform; Pulse Images.

1. **Introduction.** Textural information has become important for content-based image characterization and retrieval problems, and content-based image retrieval (CBIR) has become a popular research area in recent years due to the large amount of images in various databases[1, 2]. The issue of extracting rotation and scale invariant image features is a crucial part for any retrieval systems. Early approaches for texture retrieval and classification are second-order statistical methods, and the most popular is gray level co-occurrence matrix (GLCM) [3-5], which constructs matrices by computing the number of occurrences of pixel pairs of given quantization levels of image at given displacement and orientation values. Most popular texture extraction methods for retrieval are based on wavelet-based approaches, such as Gabor filters [6, 7], wavelets [8-10] and sub-band decomposition combined with hidden Markov model [11-13]. Texture analysis using wavelets and neural networks is proposed in [14, 15]. Although the results show that wavelet methods can achieve high accuracy rates, most of them assume that the texture images have the same orientation and scale. Since standard sub-band and wavelet decompositions are sensitive to rotation and scale, when the number of texture classes involved is large, the retrieval accuracy may drop significantly.

Besides traditional methods, pulse-coupled neural networks (PCNN) is used in texture analysis, and the output pulse images of PCNN are converted to rotation and scale invariant feature[16]. In [17], SCM is applied to invariant texture retrieval and introduce more efficient statistical measures. In this paper, SCM is applied to invariant texture retrieval on entire 112 Brodatz [18] textured images, and we explore methods of extraction features directly from DCT coefficients. The series of pulse images of SCM can be regarded as

sub-band of the original image, and present salient features such as edge, segment and texture of original images. The condensation of pulse images information into a short one-dimensional signature is a highly desirable operation. We extract robust invariant texture feature by means of computing the standard deviation of magnitude of certain DCT coefficients of the pulse images. The experimental results, based on different testing data sets for images with different orientations and scales, indicate that the proposed retrieval scheme is robust to geometrical changes, and the SCM has lower computational complexity, and obtains very high accuracy rates comparing with common methods such as Gabor, ICM and PCNN *et al.*

2. **INVARIANT TEXTURE FEATURES.** Feature extraction is a crucial step in any image retrieval systems. The extracted image features should be significant, compact and fast so that the signature is a simple and effective representation of the original image. Especially, finding an effective image feature invariant to rotation and scale is of paramount importance.

In 1990, Eckhorn *et.al.* proposed a model based on the hypothesis that neuronal pulse synchronizations can be defined as two types: stimulus-forced and stimulus-induced[19]. Stimulus-forced synchronizations are directly driven by stimulus transients and establish fast but crude sketches of association in the visual cortex, while stimulus-induced synchronizations are believed to be produced via process among local neural oscillations that are mutually connected. The feeding and linking create the membrane potential. A single feeding input of a neuron is connected to a spatially corresponding stimulus, and the linking inputs of each neuron are connected to the output of neighboring neurons within the same predetermined radius[19, 20]. Both feeding and linking are combined together as neuron's internal activity. Therefore, the SCM is described[17],

$$U_{ij}(n) = fU_{ij}(n-1) + S_{ij}\sum_{kj} W_{ijkl}Y_{ij}(n-1) + S_{ij} \tag{1}$$

$$\Theta_{ij}(n) = g\Theta_{ij}(n-1) + hY(n) \tag{2}$$

$$Y_{ij}(n) = \left\{ \begin{array}{c} 1, if U_{ij}(n) > \Theta_{ij}(n) \\ 0, otherwise \end{array} \right\} \tag{3}$$

where each neuron is denoted with indices (i, j), and one of its neighboring neurons is denoted with indices (k, l). Neuron receives input signals, and each neuron is connected to its neighbors such that the output signal of a neuron modulates the activity of its neighbors via linking synapses W. The pulse is able to fed back to modulate the threshold Θ via a leaky integrator, raising the threshold by magnitude h that decreases with time constant g. During iterations when a neuron's internal activity U exceeds its dynamic threshold Θ, pulse is generated. The SCM neuron model is shown in Fig.1.

SCM generates series of pulse images which bring out different features of original image, such as texture, edge and segment features. For an input image S, a series of pulse images $Y(1), Y(2), \ldots, Y(n)$ are outputted when SCM is iterated for n times, and the series of pulse images can be computed to a unique feature. The feature is invariant to large changes in rotation and scale of the original image[16, 17, 20] and has very strong capability to resist noise[16].

We explore DCT domain as a succeeding procedure. The DCT has the property that most of the visually significant information about the image is concentrated in just a few DCT coefficients, which inspires us to characterize the pulse images in DCT domain. The pulse images are subdivided into 8×8 pixel blocks for which information is available

in DCT domain. DC coefficient $c(1,1)$ represents the energy information. The rest of the $c(u,v)$ coefficients apart from $c(1,1)$ are called the AC coefficients, and upper left coefficients represents frequency band characteristic; upper rows, left columns and diagonal coefficients represent spatial characteristic including horizontal, vertical and diagonal patterns, respectively. The AC coefficients contain information about intensity changes within a DCT block along different orientations at different scales. Therefore, geometrical invariant texture retrieval has to extract the comprehensive characteristics of the DCT coefficients. In this paper, we select some DCT coefficients as shown in Fig.2, and such a feature vector:

$$F = [c_{11}, c_{12}, c_{13}, c_{14}, c_{15}, c_{21}, c_{22}, c_{23}, c_{24}, c_{31}, c_{32}, c_{33}, c_{34}, c_{41}, c_{42}, c_{43}, c_{44}, c_{51}] \qquad (4)$$

We extract feature by means of computing the standard deviation of magnitude of DCT coefficients. After a pulse image is transformed into DCT domain matrix, each 8×8 block has a vector F as (4), and we combine Fs together to compute the standard deviation. Therefore, for an original image, the N pulse images can be concentrated by DCT into a $1 \times N$ feature vector.

3. **EXPERIMENTAL RESULTS.** We adopt the system as shown in Fig. 3. In order to demonstrate the effectiveness of the proposed invariant feature in texture retrieval, a large number of experiments are performed with the complete set of all 112 Brodatz textured images [16]. The experiments are carried out to calculate retrieval rates using different models and different methods for images with joint rotation and scale changes. After a number of tests, we select the parameter values: internal activity initialization is set to 0 and dynamic threshold initialization to 1; f, g, and h are set to 0.2, 0.9, and 20 respectively; SCM is iterated 37 times, so the size of feature sequence is 1×37.

In the first step, we crop texture images to a standard size of $128 times 128$ and compute image signature for each images as standard database, which is performed offline. The second step is performed online, which provides user to query for image retrieval. The query image is typically different from the target image, so the retrieval methods must allow for some distortions, and we resize image by nearest neighbor interpolation then change its orientation by bilinear interpolation in this paper. We process query images to standard size of 128×128 with different orientations ($0°$ to $90°$ with $30°$ intervals) and different scales (0.8, 1 and1.2), we compare similarity by Euclidean distance between the query image and each image in the database using their signature so that the top matched images can be retrieved.

The results of invariance performance for different models and different features are summarized in Table I. SCM is compared with Gabor filter [6, 7], ICM and PCNN [16]. The results of SCM generally excel Gabor and PCNN whichever kind of signature is selected, and DCT domain features are generally better than others whichever model is selected.

Similar to experiments above, firstly, we crop images to standard size of 128×128 with different orientations ($0°$ to $90°$ with $10°$ intervals) when all are scaled up to 1.2. Secondly, we process images to standard size of 128×128 with different scales (0.6 to 1.5 with 0.1 intervals) when all are rotated 60 degrees. Fig.4 and Fig.5 show two graphs illustrating joint rotation and scale invariant retrieval results to demonstrate the capability of SCM methods. As can be seen, generally the retrieval rates decrease in turn for the following four methods: SCM, ICM, PCNN, Gabor and GLCM.

In the following experiments DCT domain feature is employed in PCNN, ICM and SCM methods. We explore that the three methods are used in invariant texture classification.

For these experiments, we prepare three different testing data sets from the Brodatz texture album. The relevant images for each query are defined as the other images with rotated and resized of original image form single region, and following [4] we evaluate the performance in terms of the average rate of retrieving relevant images as a function of the number of top retrieved images. The three testing data sets are created as follow:

For data set 1 of texture images with joint rotation and scale changes, we extract each image to size of 128×128 with different orientations (0°, 30°, 60°, and 90°) and different scales (0.6, 0.8, 1, 1.2 and 1.4). In this way, a data set of 2240 (112×4×5) texture images was created for the experiments.

For data set 2 of texture images with joint rotation and scale changes, we extract each image to size of 128×128 with different orientations (5° to 90° with 5° intervals) when all are scaled up to 1.2. In this way, a data set of 2016 (112×18) texture images was created for the experiments.

For data set 3 of texture images with joint rotation and scale changes, we extract each image to size of 128×128 with different scales (0.55 to 1.5 with 0.05 intervals) when all are rotated 60 degrees. In this way, a data set of 2240 (112×20) texture images was created for the experiments.

In order to further explain the performance, we adopt average precision and recall of the retrieval as the evaluation measures. Precision is defined as the ratio of the number of retrieved relevant images to the total number of relevant images in the whole dataset. Recall is defined as the ratio of the number of retrieved relevant images to the number of retrieved images. The experimental results are summarized in Table and Fig.6 to Fig 11, which demonstrates that the proposed methods using SCM with DCT outperform in invariant texture classification. From the table the following conclusions can be reached: Generally the SCM is of higher accuracy than PCNN and Gabor for texture classification.

4. **CONCLUSION.** We address the problem of rotation and scale invariance in texture retrieval and propose an effective DCT feature based on pulse images of SCM. The series pulse images carry abundant information about its original image, which makes it possible to apply to feature extraction. Therefore, we mainly use pulse images in invariant texture retrieval on entire 112 Brodatz textured images. The experimental results, based on different testing data sets for images with different orientations and scales, indicate that the proposed retrieval scheme using SCM is quite robust to geometrical changes and outperforms the two classic methods: Gabor filtering and the standard PCNN signature methods. The proposed schemes using pulse images of SCM are of both scale and rotation invariance. Thus, the founded SCM is a useful model for image processing and the proposed texture retrieval methods is of scale and rotation invariance. The overall retrieval accuracy of 87.5 percent for joint rotation and scale invariance is achieved with a short vector of only 37 salient features, demonstrating that the proposed method are effective joint rotation and scale invariant feature and classification accuracy over 74 percent.

REFERENCES

[1] M. S. Lew, N. Sebe, C. Djeraba, and R. Jain, Content-based multimedia information retrieval: State of the art and challenges, *ACM Trans. Multimedia Computing, Communications, and Applications*, vo. 2, no. 1, pp. 9-19, 2006.

[2] R. Datta, D. Joshi, J. Li, and J. Z. Wang, Image retrieval: Ideas, influences, and trends of the new age, *Journal of ACM Computing Surveys*, vol. 40, no. 2, pp. 1-60, 2008.

[3] R. M. Haralick, K. Shanmugam, and I. Dinstein, Textural features for image classification, *IEEE Trans. Systems, Man and Cybernetics*, vol. SMC-3, no. 6, pp. 610-621, 1973.

[4] L. K. Soh, and C. Tsatsoulis, Texture analysis of SAR sea ice imagery using gray level co-occurrence matrices, *IEEE Trans. Geoscience and Remote Sensing*, vol. 37, no. 2, pp. 780-795, 1999.

[5] D. A. Clausi, An analysis of co-occurrence texture statistics as a function of grey level quantization, *Journal of Canadian Journal of Remote Sensing*, vol. 28, no. 1, pp. 45-62, 2002.

[6] B. S. Manjunath, and W. Y. Ma, Texture features for browsing and retrieval of image data, *IEEE Trans. Pattern Analysis and Machine Intelligence*, vol. 18, no. 8, pp. 837-842, 1996.

[7] J. Han, and K. K. Ma, Rotation-invariant and scale-invariant Gabor features for texture image retrieval, *Journal of Image and Vision Computing*, vol. 25, no. 9, pp. 1474-1481, 2007.

[8] A. Laine, and J. Fan, Texture classification by wavelet packet signatures, *IEEE Trans. Pattern Analysis and Machine Intelligence*, vol. 15, no. 11, pp. 1186-1191, 1993.

[9] T. Chang, and C. C. J. Kuo, Texture analysis and classification with tree-structured wavelet transform, *IEEE Trans. Image Processing*, vol. 2, no. 4, pp. 429-441, 1993.

[10] M. N. Do, and M. Vetterli, Wavelet-based texture retrieval using generalized Gaussian density and Kullback-Leibler distance, *IEEE Trans. Image Processing*, vol. 11, no. 2, pp. 146-158, 2002.

[11] W. R. Wu, and S. C. Wei, Rotation and gray-scale transform-invariant texture classification using spiral resampling, subband decomposition, and hidden Markov model, *IEEE Trans. Image Processing*, vol. 5, no. 10, pp. 1423-1434, 1996.

[12] M. N. Do, and M. Vetterli, Rotation invariant texture characterization and retrieval using steerable wavelet-domain hidden Markov models, *IEEE Trans. Multimedia*, vol. 4, no. 4, pp. 517-527, 2002.

[13] M. N. Do, Fast approximation of Kullback-Leibler distance for dependence trees and hidden Markov models, *Journal of IEEE Signal Processing Letters*, vol. 10, no. 4, pp. 115-118, 2003.

[14] E. Avci, An expert system based on wavelet neural network-adaptive norm entropy for scale invariant texture classification, *Journal of Expert Systems with Applications*, vol. 32, no. 3, pp. 919-926, 2007.

[15] H. G. Kaganami, S. K. Ali, and Z. Beiji, Optimal approach for texture analysis and classification based on wavelet transform and neural network, *Journal of Information Hiding and Multimedia Signal Processing*, vol. 2, no. 1, pp. 33-40, 2011.

[16] J. Zhang, K. Zhan, and Y. Ma, Rotation and scale invariant antinoise PCNN features for content-based image retrieval, *Journal of Neural Network World*, vol. 17, no. 2, pp. 121-132, 2007.

[17] K. Zhan, H. Zhang, and Y. Ma, New spiking cortical model for invariant texture retrieval and image processing, *IEEE Trans. Neural Networks*, vol. 20, no. 12, pp. 1980-1986, 2009.

[18] P. Brodatz, *Textures: A photographic album for artists and designers*, Dover Publications, New York, USA, 1966.

[19] R. Eckhorn, H. J. Reitboeck, M. Arndt, and P. Dicke, Feature linking via synchronization among distributed assemblies: Simulations of results from cat visual cortex, *Journal of Neural Computation*, vol. 2, no. 3, pp. 293-307, 1990.

[20] J. L. Johnson, Pulse-coupled neural nets: translation, rotation, scale, distortion, and intensity signal invariance for images, *Journal of Applied Optics*, vol. 33, no. 26, pp. 6239-6253, 1994.

TABLE 1. comparison retrieval rates of different methods, image size is 128×128, rotation angles(r), scales(s)

scales(s)

r , s	GLCM	Gabor	Time series			Entropy			DCT		
			PCNN	ICM	SCM	PCNN	ICM	SCM	PCNN	ICM	SCM
0, 0.8	81.250	79.464	84.821	91.964	94.643	84.821	94.643	96.429	91.964	98.214	100
0, 1.0	100	100	100	100	100	100	100	100	100	100	100
0, 1.2	83.929	72.321	84.821	97.321	99.107	90.179	97.321	100	91.071	99.107	99.107
30, 0.8	36.607	41.964	55.357	68.750	69.643	64.286	75.893	76.786	71.429	75.893	87.500
30, 1.0	54.464	55.357	72.321	84.821	85.714	75.000	89.286	84.821	83.036	92.857	93.750
30, 1.2	47.321	49.107	64.286	80.357	81.143	68.750	83.036	86.607	79.464	90.179	93.750
60, 0.8	34.321	45.536	56.250	67.857	70.536	66.071	73.214	75.000	71.429	75.000	89.286
60, 1.0	45.536	55.357	72.321	84.521	84.821	75.000	89.286	85.714	85.714	91.964	95.536
60, 1.2	37.500	47.321	65.179	76.786	81.250	66.071	81.250	83.929	76.786	86.607	91.964
90, 0.8	56.250	78.571	84.821	91.864	94.643	84.821	94.643	96.429	91.964	98.214	100
90, 1.0	66.964	100	100	100	100	100	100	100	100	100	100
90, 1.2	47.321	72.321	84.821	97.321	99.107	90.179	97.321	100	91.071	99.107	99.107

TABLE 2. Comparison results of SCM with Gabor filter and PCNN

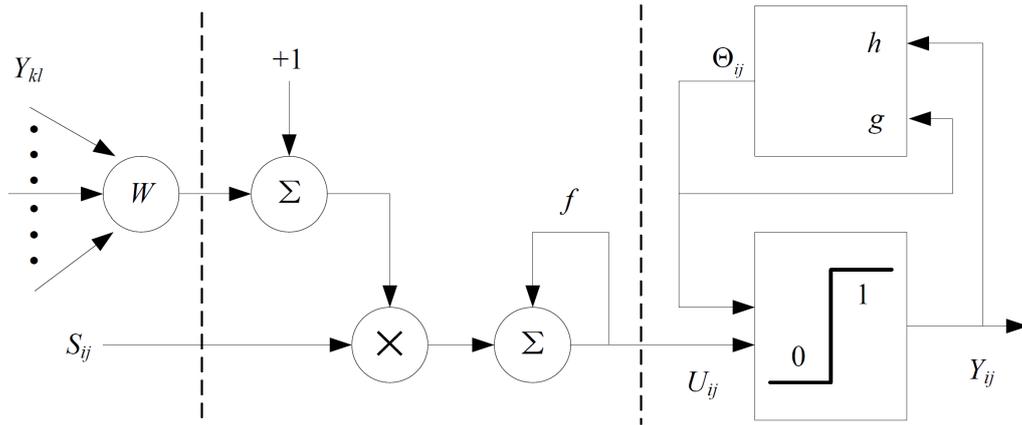|	GLCM	Gabor	PCNN	ICM	SCM
				DCT	
Data set 1	40.656	47.643	58.065	66.239	74.567
Data set 2	58.477	80.517	91.344	93.800	93.714
Data set 3	56.435	58.290	63.270	73.018	81.967

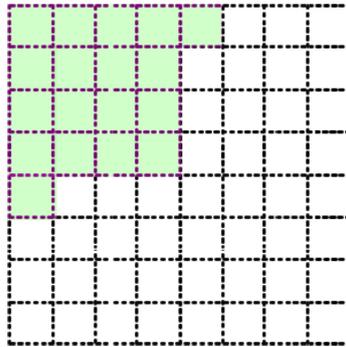FIGURE 1. The structural model illustrating SCM

FIGURE 2. Partitioning of the 8×8 DCT coefficient block into two groups for feature extraction
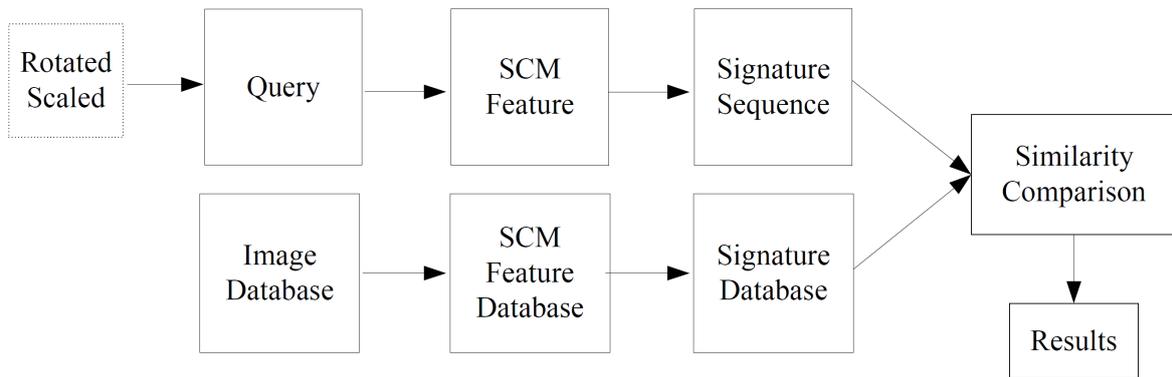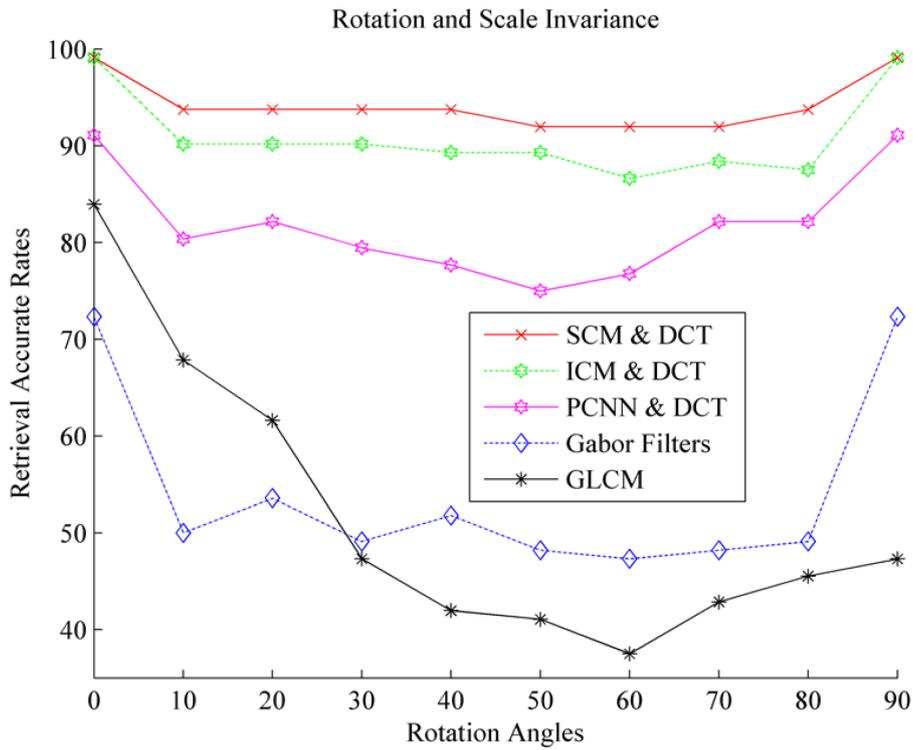

FIGURE 3. Diagram for texture retrieval

FIGURE 4. Performance of different retrieval methods using SCM, ICM, PCNN, GLCM and Gabor filter, which are subjected to different orientations when all are scaled up to 1.2
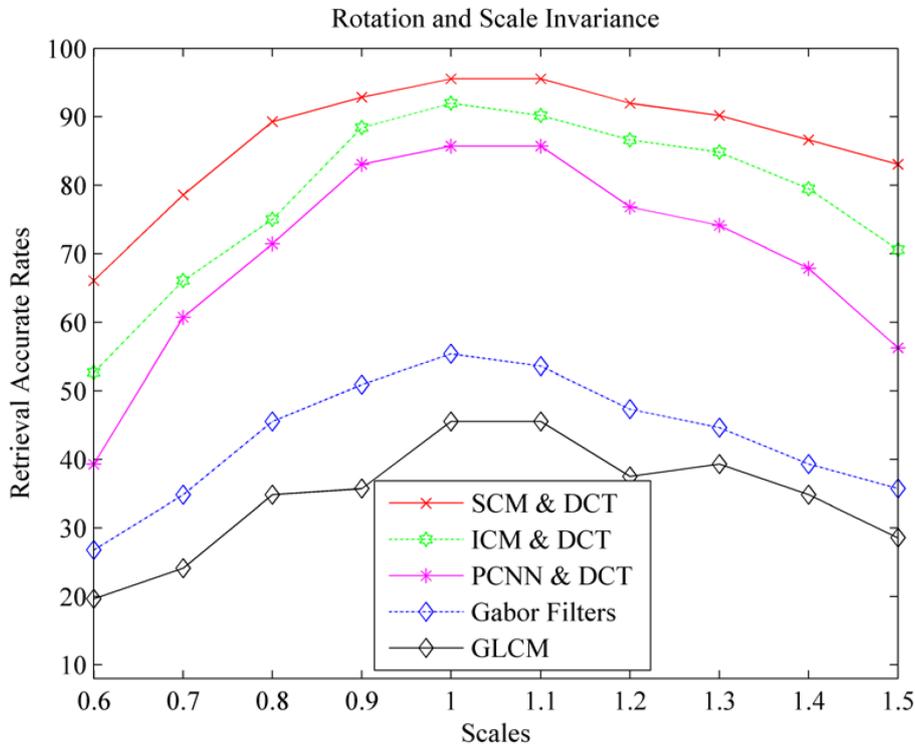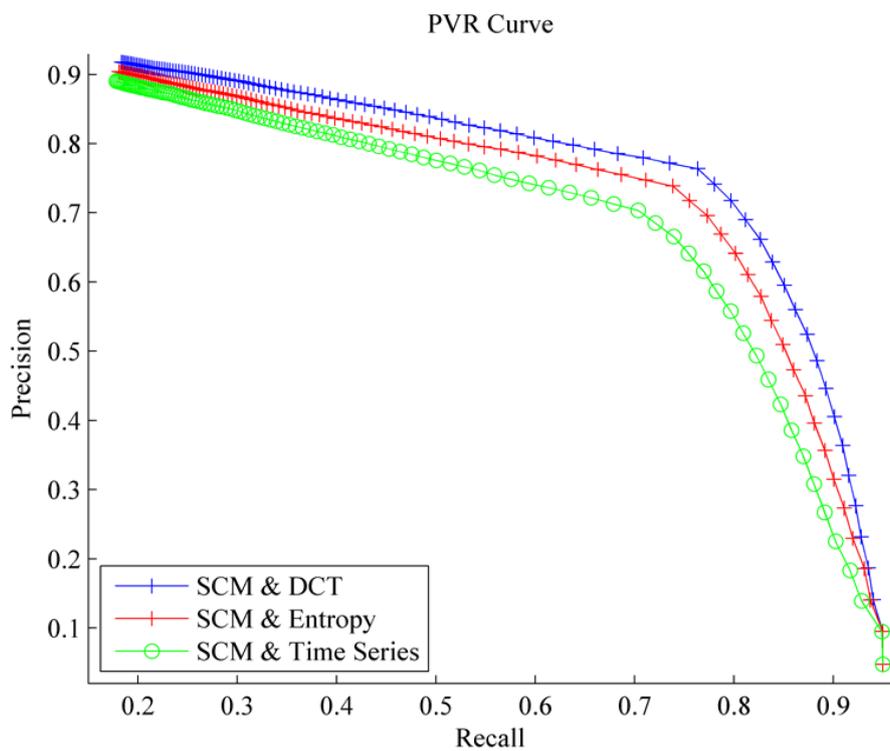

FIGURE 5. Performance of different retrieval methods using SCM, ICM, PCNN, GLCM, and Gabor filter, which are subjected to different scales when all are rotated 60 degrees
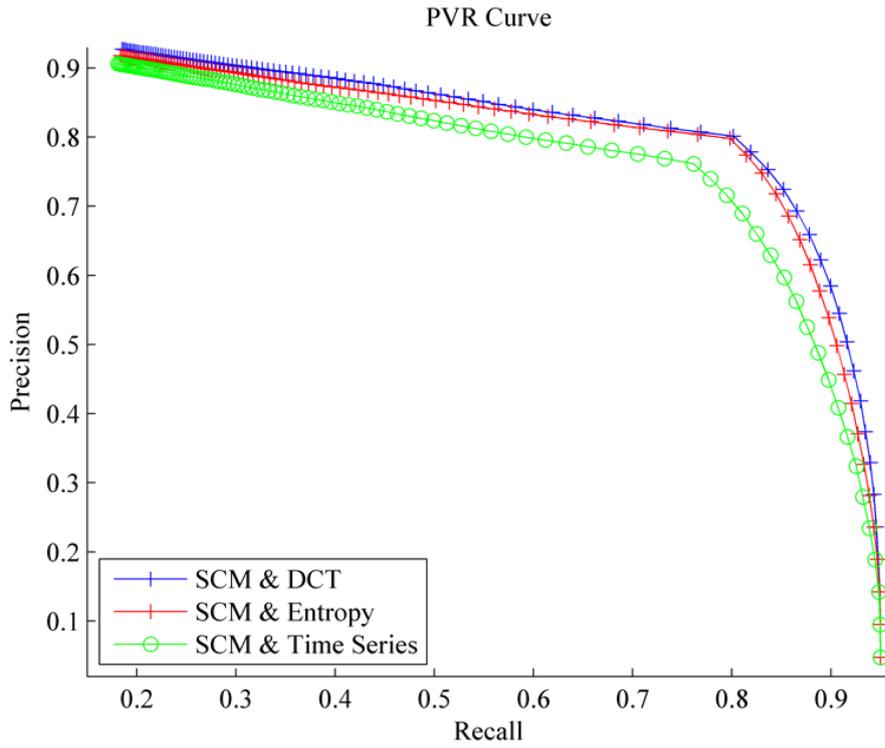
FIGURE 6. Average retrieval precision-recall for data set 1 using SCM with different features
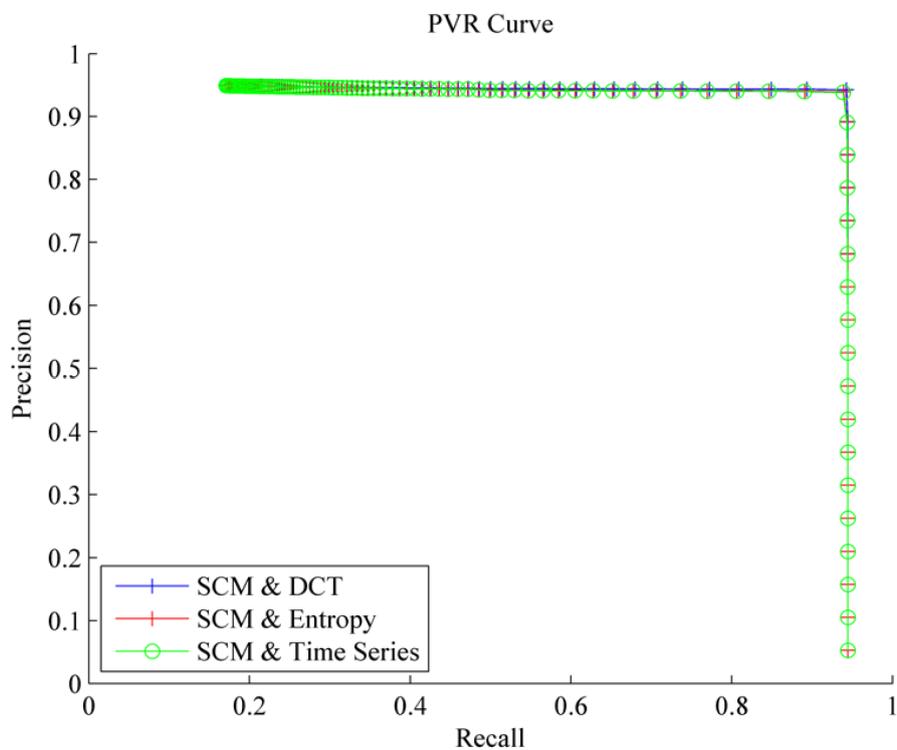
FIGURE 7. Average retrieval precision-recall for data set 2 using SCM with different features

FIGURE 8. Average retrieval precision-recall for data set 3 using SCM with different features
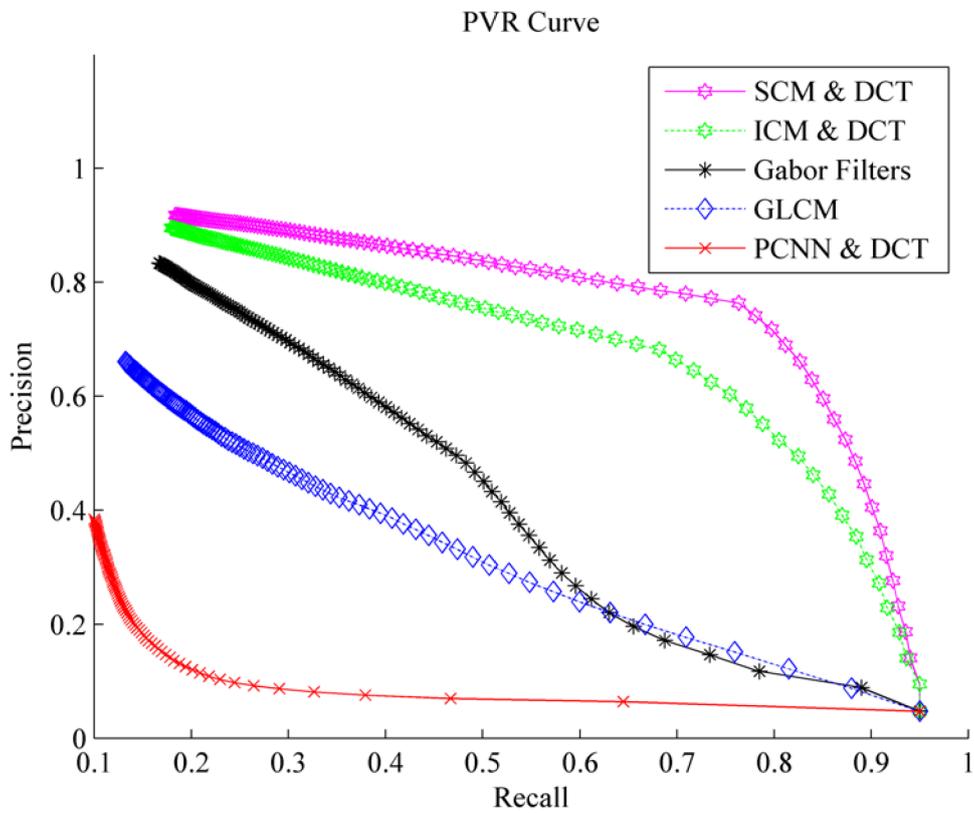

FIGURE 9. Average retrieval precision-recall for data set 1 using SCM, ICM, PCNN, GLCM, and Gabor filter
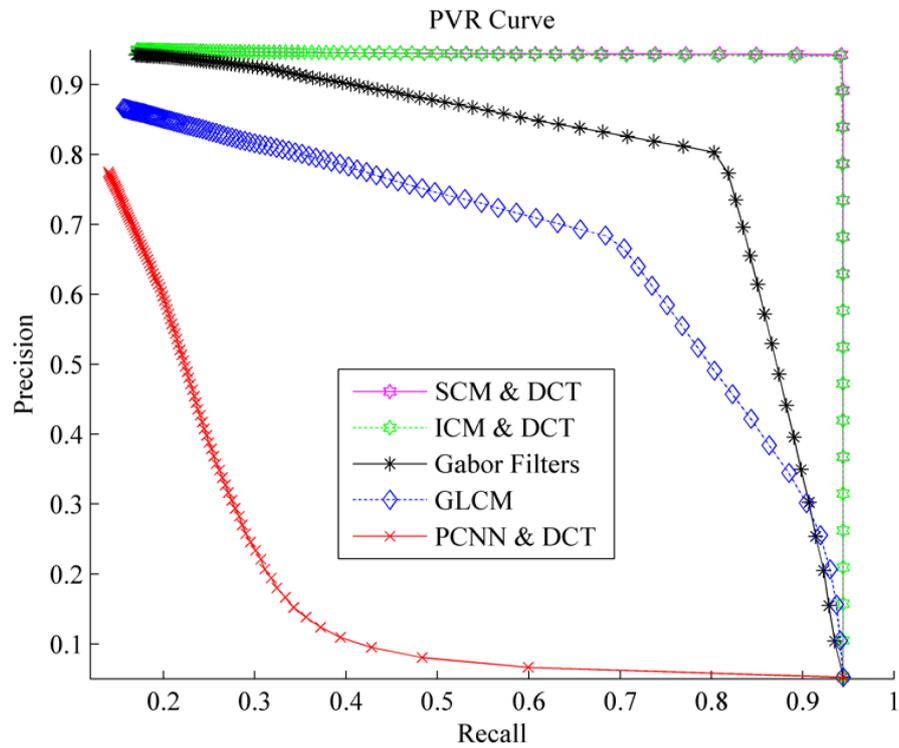
FIGURE 10. Average retrieval precision-recall for data set 2 using SCM, ICM, PCNN, GLCM, and Gabor filter
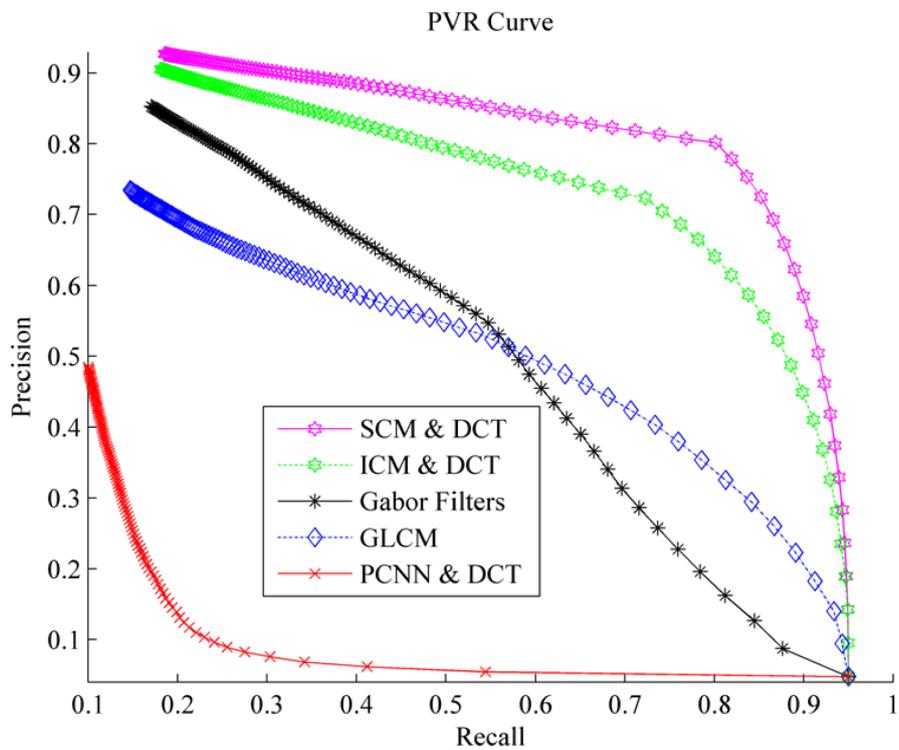

FIGURE 11. Average retrieval precision-recall for data set 3 using SCM, ICM, PCNN, GLCM, and Gabor filter